# Measurement and Analysis of Radio Frequency Interference in the UWB Spectrum

Adeogun, Ramoni Ojekunle; Berardinelli, Gilberto; Rodriguez, Ignacio; E. Mogensen, Preben; Razzaghpour, Mohammad

*Published in:*
2019 IEEE 90th Vehicular Technology Conference (VTC2019-Fall)

*DOI (link to publication from Publisher):*
10.1109/VTCFall.2019.8891426

*Publication date:*
2019

*Document Version*
Accepted author manuscript, peer reviewed version

# Measurement and Analysis of Radio Frequency Interference in the UWB Spectrum

Ramoni Adeogun*, Gilberto Berardinelli*, Ignacio Rodriguez*, Preben Elgaard Mogensen*† and Mohammad Razzaghpour*
*Wireless Communication Networks Section, Department of Electronic Systems, Aalborg University, Denmark
† Nokia Bell Labs, Aalborg, Denmark
E-mail:[ra, gb, irl,pm mor]@es.aau.dk

***Abstract*—Ultra-wide band (UWB) radio systems are expected to operate in co-existence with a myriad of other systems over a large unlicensed bandwidth. Thus, UWB devices need to incorporate efficient inter-system interference mitigation mechanisms. In this paper, we present interference measurements covering the UWB spectrum from 3 GHz to 11 GHz conducted at two locations (indoor and outdoor) on the campus of Aalborg University, Denmark. We analysed the measurements in terms of occurrence probability, interference power distribution and inter-arrival time statistics. The goal is to understand the characteristics of signals emanating from systems operating on this ultra-wide bandwidth as a basis for the development of models and methods for interference characterization and mitigation. Results indicate that signal activity vary significantly across the spectrum with the 5 GHz – 6 GHz and 9 GHz – 10 GHz sub-bands having the strongest power levels in the indoor and outdoor measurements, respectively. Statistical analysis results further show significant variation of the power distribution, occurrence probability and inter-arrival time statistics for the various signals detected in the measurements. Results also show that time between interference occurrence is exponentially distributed for most of the sources.**

***Index Terms*—UWB, modelling, wireless systems, interference measurements, spectrum sensing**

## I. Introduction

UWB technology enables low power, short range communication over a large part of the radio spectrum. The definition of UWB relates to the transmitted signal bandwidth. For instance, the Federal Communications Commission (FCC) classified a technology as UWB if the signal bandwidth is greater than 500 MHz or its fractional bandwidth is a minimum of 20 % of the carrier frequency in the United States. On the other hand, the European commission specified a minimum bandwidth of 50 MHz for UWB communications [1]. In general, unlicensed access is given for ultra-wideband communications over a large spectrum in the range 3.1 to 10.6 GHz, with tight restrictions in terms of power spectral density (PSD).

The restrictions on transmission power limit the amount of interference from UWB devices to other co-existing users. However, UWB devices may experience significant interference from a myriad of licensed and unlicensed sources such as WIreless Local Area Network (WLAN), Worldwide Interoperability for Microwave Access (WiMAX), radiolocation, and satellite systems in the large spectrum. For instance, WLAN devices can occupy part of the channels in the 5 GHz Unlicensed National Information Infrastructure (UNII) band with much higher maximum effective radiated power (ERP) compared to the PSD limit of -41.3 dBm/MHz for UWB communication. Interference from WLAN devices may therefore be very strong depending on the device separation distance necessitating the need to incorporate appropriate interference mitigation and/or avoidance techniques in UWB devices. Recent studies have also identified UWB as a candidate solution for wireless communications in industrial scenarios , see e.g., [2] and the references therein.

There has been considerable amount of research works on interference from UWB devices to other co-exisiting systems such as IEEE 802.11x (WiFi), WiMAX and Global Positioning System (GPS), see e.g., [3]–[7] and the references therein. However, investigations on the interference to UWB systems have been mostly focused on performance evaluations and receiver processing techniques for specific UWB transmission technologies. A coherent rake receiver to mitigate multiuser interference (MUI) in impulse radio UWB (IR-UWB) is proposed in [4]. Similar studies on interference analysis and mitigation have also been reported in [8]–[10]. On the other hand, studies on characterization and/or modelling of interference over the entire UWB system have been majorly limited to intra-system inteference in multiuser scenarios. For instance, approximations for multiuser interference in time hopping-UWB using Gaussian mixture distribution, Middleton class A noise and the Laplace distribution are investigated in [11] based on bit error rate performance simulations. Moreover, there is no study in the open literature on characterization of interference in the entire UWB spectrum based on measurements, to the best knowledge of the authors.

In this paper, we present results of our first set of interference measurements in the UWB spectrum. Interference measurements were performed at an indoor and a outdoor location on the campus of Aalborg University, Denmark. We study the distributions of radio frequency interference (RFI) power and the time between RFI occurrence on sub-bands where significant interference is detected in the measurements. The goal is to understand, quantify and characterize the potential interference signals from systems in the entire UWB spectral range. The key contributions of this paper are as follows:

- We performed interference measurements covering the entire UWB frequency range from 3 GHz to 11 GHz at an indoor and a outdoor location. The measurements were

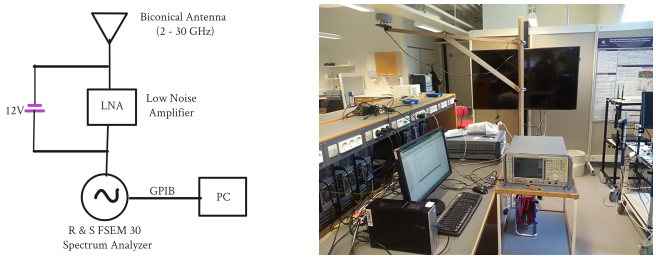


(a) Set up. (b) Image from WCN Lab.

Fig. 1: UWB RFI measurement set up.

conducted to set the framework for UWB spectrum sensing and to study the temporal and frequency dynamics of signal activities on the ultra-wide spectrum. To the best knowledge of the authors, this is the first measurement based study over the entire UWB spectrum and can therefore be used as basis for further measurements and to gain insights into expected behaviour of signals on this ultra-wide spectrum.

- We analysed the measurements in terms of probability of interference occurrence per 500 MHz sub-bands, RFI power distribution and inter-arrival time statistics.

## II. Measurement Procedure

The RFI measurement system, shown in Fig. 1 comprises of; a $2-30\,\mathrm{GHz}$ bi-conical antenna, a $2-18\,\mathrm{GHz}$ Low Noise Broadband Amplifier (LNBA)[1] with $26\,\mathrm{dB}$ gain/3 dB noise figure, and an R & S FSEM 30 spectrum analyzer with frequency range, 20 Hz - 26.5 GHz and resolution bandwidth (RBW) of 10 Hz - 10 MHz. The spectrum analyzer is remotely controlled for measurement and data recording by a computer, which is connected to the General Purpose Interface Bus (GPIB) interface using National Instruments GPIB-USB-B interface adapter.

The spectrum sensing was performed following International Telecommunication Union (ITU)'s recommendations for UWB peak radiated power measurements [12], [13] with a RBW and video bandwidth (VBW) of 1 MHz. The center frequency and span were set to cover 8 GHz bandwidth from 3 GHz to 11 GHz. The detector and Max Hold functionalities of the analyzer were set to Peak and ON, respectively.

Measurements were conducted in the Wireless Communication Networks (WCN) lab and on the roof top of the Fredrik Bajers vej building at Aalborg University campus. This is to aid identification of potential interference sources via comparison of the indoor and outdoor interference power levels. The WCN lab has a number of work spaces and equipment, which are used for experimental research activities. The lab also houses CISCO routers and switches based experimental IP networks that can be accessed via multiple technologies including Bluetooth, and IEEE 802.11a/b/g WLAN.

[1]The LNA is powered by the main power supply via a 12V AC-DC converter.

TABLE I: Potential sources of interference to systems operating on the UWB spectrum in Denmark. Extracted from the Danish Energy Agency's frequency allocation register [14].

| SN | Freq. [MHz] | Type of Primary Systems |
|---|---|---|
| I | 3250 | Satellite; |
| II | 3750 | Satellite; Radiolink, point-to-point |
| III | 4250 | Satellite |
| IV | 4750 | - |
| V | 5250 | Satellite |
| VI | 5750 | Radar; Landmobile; Fixed Wireless Access (FWA); Satellite |
| VII | 6250 | Satellite; Fixed Wireless Access (FWA); Radiolink, point-to-point |
| VIII | 6750 | Radiolink, point-to-point |
| IX | 7250 | Radiolink, point-to-point |
| X | 7750 | Radiolink, point-to-point |
| XI | 8250 | - |
| XII | 8750 | - |
| XIII | 9250 | Radar |
| XIV | 9750 | Radar |
| XV | 10250 | Radar; radiolink, point-to-point; Fixed Wireless Access |
| XVI | 10750 | Radiolink, point-to-point |

TABLE II: Parameter of fitted exponential distributions to measured RFI inter-arrival times.

| Indoor (WCN Lab) | | | Outdoor (Roof Top) | | |
|---|---|---|---|---|---|
| Freq [MHz] | Rate ($\lambda$) | 95% Conf. Interval | Freq [MHz] | Rate ($\lambda$) | 95% Conf. Interval |
| 5196 | 11.32 | [11.08 11.58] | 3577 | 1.58 | [1.57 1.59] |
| 5244 | 494.25 | [428.48 576.50] | 9365 | 93.50 | [87.76 99.83] |
| 5325 | 29.57 | [28.53 30.67] | 9541 | 246.20 | [222.09 274.49] |
| 5533 | 15.07 | [14.69 15.47] | 9717 | 143.94 | [132.87 156.45] |
| 5693 | 16.17 | [15.75 16.62] | 9766 | 105.76 | [98.86 113.41] |
| 7665 | 493.81 | [427.59 576.79] | 9862 | 132.05 | [122.49 142.79] |
| 10407 | 66.94 | [63.44 70.74] | 9910 | 116.86 | [108.90 125.81] |

The measurements reported in this paper consist of 55000 consecutive sweep of the entire 3 GHz to 11 GHz spectrum over a duration of 24 hours with RBW and VBW of 1 MHz. The sweep time was manually set to 1 s and a delay of approximately 500 ms[2] was introduced between sweeps to account for the delay associated with data transmission and re-initialization of the spectrum analyzer. The maximum peak detector of the analyzer is used for all measurements. A total of 500 equally spaced discrete samples (i.e., bins) were recorded over the 8 GHz frequency span. Therefore, the analyzer measures from the start frequency to the stop frequency and assign to each frequency point, the maximum power level detected within the 16 MHz bin during each sweep operation.

## III. Measurement Results and Statistical Analysis

We discuss the measurements and analyze the measurements using occurrence probability as well as statistical distribution of RFI power levels and the inter-arrival time in this section. To aid discussion of the measurements, we present a summary of spectrum allocations by the Danish Energy Agency in the 3 GHz to 11 GHz spectral range in Table I. Considering the very wide bandwidth and for clarity of presentation, we divided the 8 GHz band into 16 sub-bands with 500 MHz size. The table shows that the UWB spectrum accommodates different systems including satellite, radar, point-to-point, and Fixed Wireless Access (FWA) and hence, different signal

[2]Note that this delay may result in some of the signals not been detected and can be avoided via zero-span measurements. However, it is quite unlikely that a specific signal will be missed during all sweeps over the 24 hours duration. An alternative approach is to divide the 8 GHz into smaller chunks and perform measurement over each chunk separately.

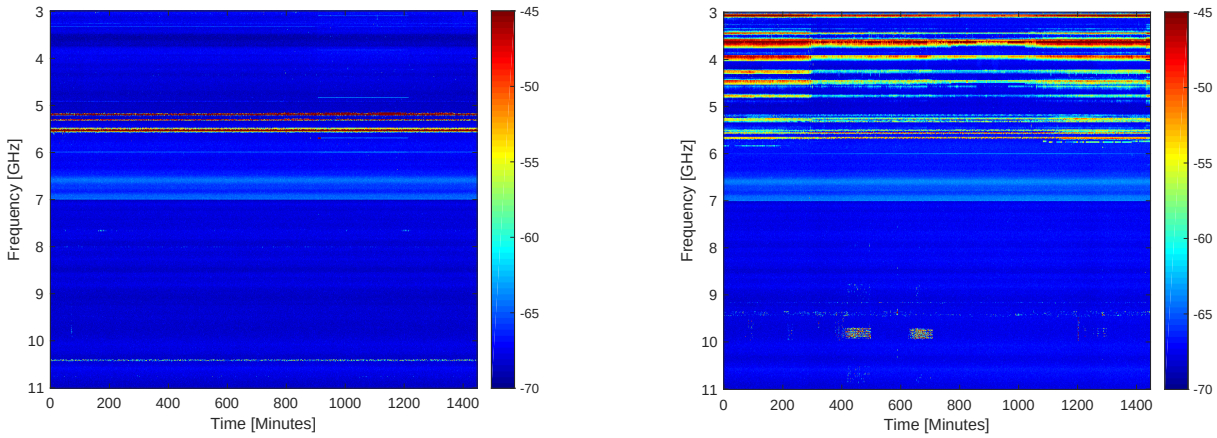


(a) WCN Lab.

(b) FRB7 Roof Top.

Fig. 2: Spectrogram of UWB RFI obtained from measurements at WCN Lab and FRB7 roof top.

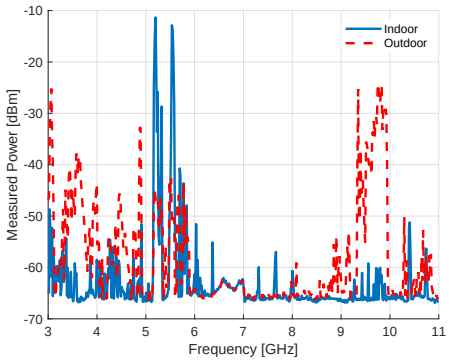


Fig. 3: UWB Radio Frequency Interference Profile (RFI) obtained from indoor and outdoor measurements.

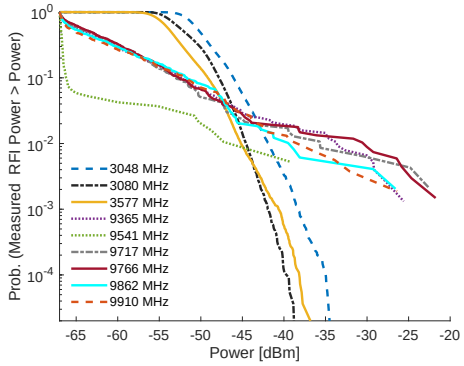


Fig. 5: Measured power level probability distributions for selected interference sources from data obtained in the roof top.

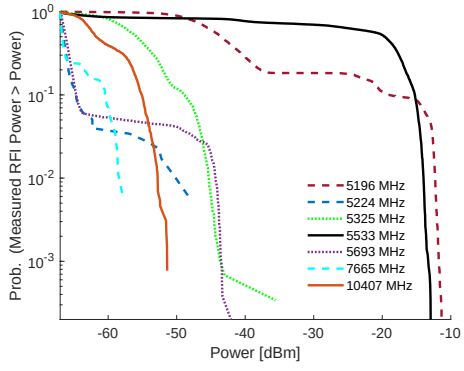


Fig. 4: Measured power level probability distributions for selected interference sources from data obtained in the WCN lab.

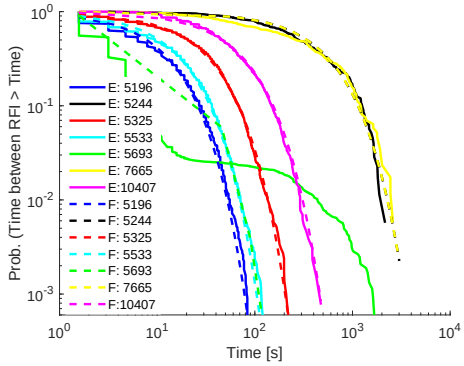


Fig. 6: Emprical RFI inter-arrival time (solid lines) and fitted exponential distributions (dashed lines) for selected interference sources from data obtained in the WCN lab. Parameter of fitted distributions are presented in Tab. II.

characteristics are expected. Note that the sub-bands in the 5 GHz – 6 GHz frequency range also houses the popular IEEE 802.11x occupying different parts of UNII channels.

### A. *RFI Measurements*

Fig. 2 presents the measured spectrograms over a period of 24 hours for both locations. In the indoor measurement (Fig. 2a), signals detected between 5 GHz and 6 GHz appears to be persistent over the entire duration. Similar continuous signal activity is seen between 3 GHz and 6 GHz in the outdoor spectrogram in Fig. 2b. In Fig 2b, the sources be-

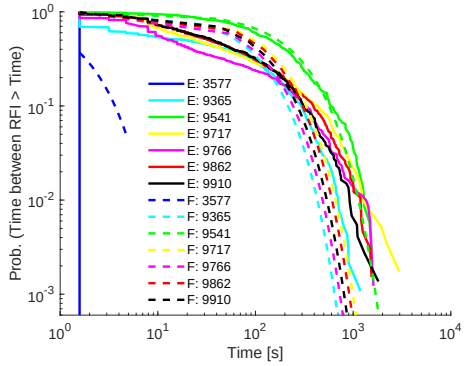


Fig. 7: Emprical RFI inter-arrival time (solid lines) and fitted exponential distributions (dashed lines) for selected interference sources from data obtained on the roof top. Parameter of fitted distributions are presented in Tab. II.

TABLE III: Averaged interference probabilities for 16 500 MHz sub-bands on the 8 GHz UWB spectrum. Modelled for interference sources with detected power $\geq$-60 dBm.

| **Freq. [GHz]** | Probability (%) | | | | | | | | | |
|---|---|---|---|---|---|---|---|---|---|---|
| | Indoor | | | | | Outdoor | | | | |
| | N | Min. | Mean | Max | STD. | N | Min. | Mean | Max | STD. |
| 3.25 | 9 | 0.002 | 0.004 | 0.013 | 0.004 | 27 | 0.002 | 17.081 | 99.878 | 33.934 |
| 3.75 | 3 | 0.002 | 0.002 | 0.002 | 0 | 30 | 0.004 | 37.494 | 99.818 | 38.135 |
| 4.25 | 9 | 0.002 | 0.003 | 0.006 | 0.001 | 24 | 0.002 | 8.597 | 34.180 | 11.341 |
| 4.75 | 2 | 0.002 | 0.002 | 0.0028 | 0 | 18 | 0.002 | 2.018 | 10.940 | 3.356 |
| 5.25 | 12 | 0.002 | 3.335 | 13.762 | 4.010 | 20 | 0.002 | 1.684 | 7.787 | 2.550 |
| 5.75 | 15 | 0.002 | 2.740 | 9.015 | 3.811 | 23 | 0.002 | 2.614 | 16.375 | 3.961 |
| 6.25 | 3 | 0.002 | 0.002 | 0.002 | 0 | 0 | 0 | 0 | 0 | 0 |
| 6.75 | 0 | 0 | 0 | 0 | 0 | 2 | 0.002 | 0.002 | 0.002 | 0 |
| 7.25 | 1 | 0.002 | 0.002 | 0.002 | 0 | 0 | 0 | 0 | 0 | 0 |
| 7.75 | 2 | 0.009 | 0.016 | 0.024 | 0.010 | 3 | 0.002 | 0.002 | 0.002 | 0 |
| 8.25 | 0 | 0 | 0 | 0 | 0 | 2 | 0.002 | 0.003 | 0.004 | 0.001 |
| 8.75 | 0 | 0 | 0 | 0 | 0 | 12 | 0.002 | 0.004 | 0.011 | 0.003 |
| 9.25 | 0 | 0 | 0 | 0 | 0 | 15 | 0.002 | 0.078 | 0.406 | 0.129 |
| 9.75 | 1 | 0.002 | 0.002 | 0.002 | 0 | 28 | 0.004 | 0.142 | 0.400 | 0.140 |
| 10.25 | 3 | 0.004 | 0.618 | 0.926 | 0.531 | 4 | 0.002 | 0.003 | 0.004 | 0.001 |
| 10.75 | 2 | 0.002 | 0.010 | 0.018 | 0.012 | 16 | 0.002 | 0.005 | 0.015 | 0.004 |

tween 9 GHz and 10 GHz are however intermittent with two occurrences over the 24 hour period.

The RFI spectra observed at the two measurement locations are shown in Fig. 3, where we plot the maximum of all RFI samples at each frequency point over the entire 24 hours duration. It can be seen from the figure that interference power levels vary significantly across the UWB spectrum in both indoor and outdoor locations. In both locations, the sub-band from 6 GHz to 9 GHz shows relatively low signal activity indicating the presence of few potential interference sources in this sub-band. From the indoor measurements, the 5 GHz to 6 GHz band is observed to have the highest interference power levels. This is most likely due to the presence of a WiFi router and devices utilizing WiFi connectivity in the lab. Considering the measured power level in this frequency range, it is quite unlikely that the detected RFIs are from any other sources (i.e., satellite or radar) than WiFi. However, this does not eliminate the possibility of picking up weaker interference signals from other sources in indoor environments. On the other hand, the most significant interferers occupy the 9 – 10 GHz range in the outdoor measurements. Considering the spectrum allocations in Table I, signals in this frequency range are most likely from radar systems.

### *B. RFI Statistics*

Since the peak detector of the spectrum analyzer was used during the measurements, only the maximum power of the RFI within each bin is recorded. The measured peak power levels can be used to study the statistical distributions of RFI power and the time spacing between interference occurrence. In this section, we characterize the measured RFI power levels and inter-arrival times. Statistical model for inter-arrival times is also presented via empirical fitting of the exponential distributions.

Let $I_o$ denote a specific interference power level, we define the Interference Power Distribution, IPD($I_o$), as the probability that a measured RFI power exceeds $I_o$. Thus

$$\begin{aligned} \text{IPD}(I_o) &= \text{Probability}[I \geq I_o] \\ &= 1 - \text{CDF}(I_o), \end{aligned} \tag{1}$$

where CDF($I_o$) denotes the cumulative distribution function.

We present the IPD for selected RFI obtained from the indoor- and outdoor measurements in Fig. 4 and Fig. 5, respectively. Fig. 4 shows that two RFIs detected at 5196 MHz and 5533 MHz have the strongest power levels of approximately -11 dBm and -13 dBm, respectively. The RFI source detected at 5533 MHz appear to have a consistently strong power with approximately 90% probability that its power is above -15 dBm. Compared to these two sources, other RFIs detected have much lower power with the ones at 5325 MHz and 5693 MHz having a maximum power level of about -40 dBm.

In Fig. 5, we observe that all RFIs in the 9 GHz - 10 GHz range have similar IPD except for the interference source at 9541 MHz. This similarity is not surprising since all RFIs in this range are most likely radar signals as shown in Table I.

We present the distribution of the time between RFIs occurrence for the indoor and outdoor measurements in Fig. 6 and Fig. 7, respectively. In Fig. 6, we observe that the RFIs at 5196 MHz and 5533 MHz have similar exponential RFI spacing distribution with a maximum time between interference occurrence of approximately 100 seconds. This observation coupled with similarity in power level statistics indicate that these two interferers are different channels of the 5 GHz WLAN. Therefore, as expected, the major interference sources that any UWB based system has to contend with in the measured indoor environments are the 5 GHz WLAN (i.e., WiFi) channels. This raises concerns about whether WiFi channels should be completely avoided in the design of wireless systems that opportunistically utilize the UWB spectrum. In order to address this concern, more measurements needs to be conducted to verify the generality of this observation and obtain representative interference patterns. Furthermore, the RFIs detected at 5244 MHz and 7665 MHz also show similar RFI spacing distribution. Except for the source at 5693 MHz,

fitted exponential curves match closely with the empirical distributions.

Similarly, inter-arrival time of all RFIs detected in the outdoor measurement are also exponentially distributed as shown in Fig. 7 except for the signal in the 3 GHz to 4 GHz frequency range for which the distribution of inter-arrival time is a vertical line at the sampling interval of our measurements (approximately 1.5 seconds). As seen in Fig. 2b, sources in this frequency range exhibit continuous activity over the entire measurement period. Therefore, a plausible conclusion is that the sampling interval in our measurement is much higher than the spacing between occurrence of these signals and that improved time resolution is required to estimate the inter-arrival times of these RFIs.

The results so far show significant variations in the interference power levels and occurence time over the entire UWB spectrum. We now present results quantifying signal activity in each 500 MHz sub-band in Table III, where we show the number of frequency points and statistics (mean, minimum, maximum and standard deviation) of the probability that a frequency point experiences interference power level above -60 dBm, i.e., approximately 7 dBm above the displayed noise floor in the measurements. Denoting the number of frequency points within each sub-band as N, the probability is computed using [15]

$$p_n = \frac{\sum_{m=1}^{M_n} \mathcal{X}(I_n(m))}{M_n}; \quad n = 1, 2, \cdots, N \tag{2}$$

where

$$\mathcal{X}(I_n) = \begin{cases} 1 & \text{if } I_n > -60\,\text{dBm} \\ 0 & \text{if } I_n \leq -60\,\text{dBm}, \end{cases}$$

$I_n$ and $M_n$ are the RFI power levels and number of RFI samples at the $n$th frequency point. The table shows that the number of interfered frequency locations within each 500 MHz band is much higher in the outdoor measurements. This is expected since most of the potential interference signals in these bands are either from satellite or radar systems which will have much weaker power level in an indoor environment than outdoor due to penetration as well as distant dependent losses. The occurrence probabilities also vary significantly even for sources within some of the 500 MHz sub-bands. For the indoor measurements, the highest occurrence probability values are approximately 14% and 9% for the sub-bands centred at 5.25 GHz and 5.75 GHz, respectively. Thus, in the 5 GHz – 6 GHz and 9 GHz – 10 GHz sub-bands, where the strongest interference powers are seen in Fig. 3, signal activity is less than 15% and 1%, respectively. This indicates the potential for opportunistic usage of the most interfered bands.

## IV. Summary and Conclusion

We performed measurements to characterize signal activity and temporal dynamics of radio frequency interference from systems operating on the $3-11$ GHz UWB spectrum. Results from both outdoor and indoor locations indicate significant variation in signal activity over the UWB spectrum. In the 5 GHz – 6 GHz and 9 GHz – 10 GHz sub-bands, where the strongest interference powers were detected, signal activity over the entire duration of the measurements is relatively low with maximum occurrence probability of approximately 15% and 1%, respectively. Statistical analysis results indicated that the distributions of interference power and inter-arrival times vary across the spectrum. For these measurements, the inter-arrival times of the detected signals are exponentially distributed. Our ongoing research is conducting further interference measurements to generalize observations from the preliminary measurements and develop models for interference signals in the UWB spectrum.

## References


[1] V. Niemel, J. Haapola, M. Hmlinen, and J. Iinatti, "An ultra wideband survey: Global regulations and impulse radio research based on standards," *IEEE Communications Surveys Tutorials*, vol. 19, no. 2, pp. 874–890, Secondquarter 2017.

[2] G. Berardinelli, N. H. Mahmood, I. Rodriguez, and P. Mogensen, "Beyond 5G Wireless IRT for Industry 4.0: Design Principles and Spectrum Aspects," in *2018 IEEE Globecom Workshops (GC Wkshps)*, Dec 2018, pp. 1–6.

[3] H.-J. Song, D.-K. Kim, M.-J. Kim, and H.-S. Lee, "A study of the interference measurement analysis between SDMB system and UWB wireless communication system," in *The 7th International Conference on Advanced Communication Technology, 2005, ICACT 2005.*, vol. 2, Feb 2005, pp. 1117–1120.

[4] M. Flury and J. L. Boudec, "Interference Mitigation by Statistical Interference Modeling in an Impulse Radio UWB Receiver," in *2006 IEEE International Conference on Ultra-Wideband*, Sep. 2006, pp. 393–398.

[5] E. M. Shaheen and M. El-Tanany, "The impact of narrowband interference on the performance of UWB systems in the IEEE802.15.3a channel models," in *CCECE 2010*, May 2010, pp. 1–6.

[6] V. Cellini and G. Dona, "A novel joint channel and multi-user interference statistics estimator for UWB-IR based on Gaussian mixture model," in *2005 IEEE International Conference on Ultra-Wideband*, Sep. 2005, pp. 655–660.

[7] S. Kandeepan, G. Baldini, and R. Piesiewicz, "Preliminary experimental results on the spectrum sensing performances for UWB-Cognitive Radios for detecting IEEE 802.11n systems," in *2009 6th International Symposium on Wireless Communication Systems*, Sep. 2009, pp. 111–115.

[8] S. V. Mir-Moghtadaei, A. Z. Nezhad, and A. Fotowat-Ahmady, "A new IR-UWB pulse to mitigate coexistence issues of UWB and narrowband systems," in *2013 21st Iranian Conference on Electrical Engineering (ICEE)*, May 2013, pp. 1–5.

[9] B. Das and S. Das, "Interference mitigation techniques in transmitted reference UWB system used in WPANs NLOS channel environment," in *2010 Annual IEEE India Conference (INDICON)*, Dec 2010, pp. 1–4.

[10] C. Zhang, H. Yin, and P. Ren, "The Effects of Narrowband Interference on Finite-Resolution IR-UWB Digital Receivers," *IEEE Communications Letters*, vol. 15, no. 5, pp. 536–538, May 2011.

[11] B. Hu and N. C. Beaulieu, "On characterizing multiple access interference in TH-UWB systems with impulsive noise models," in *2008 IEEE Radio and Wireless Symposium*, Jan 2008, pp. 879–882.

[12] I.-R. SM.1754-0, "Measurement techniques of ultra-wideband transmissions," International Telecommunications Union, Tech. Rep., 2006.

[13] I. Shinobu, G.Kaoru, Y. Yukio, and M. Yasushi, "Power Measurement Emitted by UWB System in Time Domain," *Journal of the National Institute of Information and Communications Technology*, vol. 53, no. 1, pp. 91–99, 2006.

[14] D. E. Agency. (2019) Frequency Register: Reporting of frequency permits and call signals. [Online]. Available: https://frekvensregister.ens.dk/Search/Search.aspx

[15] M. Lauridsen, B. Vejlgaard, I. Z. Kovacs, H. Nguyen, and P. Mogensen, "Interference Measurements in the European 868 MHz ISM Band with Focus on LoRa and SigFox," in *2017 IEEE Wireless Communications and Networking Conference (WCNC)*, March 2017, pp. 1–6.